# Orientation effects of deformed nuclei on the production of superheavy elements

Nan Wang,[1] Jun-qing Li,[2,4] and En-guang Zhao[3,4]
[1]*College of Physics, Shenzhen University, Shenzhen 518060, People's Republic of China*
[2]*Institute of Modern Physics, The Chinese Academy of Sciences, Lanzhou 730000, People's Republic of China*
[3]*Institute of Theoretical Physics, The Chinese Academy of Sciences, Beijing 100190, People's Republic of China*
[4]*Center of Theoretical Nuclear Physics, National Laboratory of Heavy ion Accelerator, Lanzhou 730000, People's Republic of China*
(Received 14 July 2008; revised manuscript received 22 September 2008; published 24 November 2008)

Within the dinuclear system model, the effects of the relative orientations of interacting deformed nuclei on the interaction potential energy surfaces, the evaporation residue cross sections of some cold fusion reactions leading to superheavy elements are investigated. The competition between fusion and quasifission is studied to show the effect of the orientation. It turns out that the belly-belly orientation is in favor of the production of superheavy nuclei, because in the case a barrier has suppressed the quasifission and thus helped fusion.

DOI: 10.1103/PhysRevC.78.054607 PACS number(s): 25.70.Jj, 24.10.−i, 25.60.Pj

## I. INTRODUCTION

The exploration of synthesis of superheavy elements (charge number $Z \geqslant 106$) is hotly maintained in both experimental and theoretical aspects. The superheavy nuclei can exist against the strong Coulomb repulsion because of the existence of the shell effect. Some cold fusion reactions with the target Pb or Bi are performed to produce the superheavy nuclei $Z = 107$–$112$ [1], and some superheavy nuclei are produced with hot fusion that some actinide nuclei are bombarded by doubly magic nucleus $^{48}$Ca [2]. In the theoretical aspect, to understand the production mechanism of superheavy nucleus (SHN), several models are proposed, such as the dinuclear system (DNS) concept, the fluctuation-dissipation model, the nuclear collectivization concept, as well as the macroscopic dynamical model [3–13]. Although great achievements about understanding the production mechanism of SHN have been obtained, there are still many problems that are not fully understood. The reasonable understanding of the formation of superheavy nuclei is still a challenge for the theory.

The present work is based on the DNS model. After the capture process, the DNS system is formed in the pocket of the nucleus-nucleus potential. The compound nucleus is formed by successive nucleon transfer from one nucleus to the other until all the nucleons of the smaller nucleus emerged in the larger one. The transfer process has to pass over the inner fusion barrier. Meanwhile, two nuclei at any mass asymmetry may overcome a barrier along the distance $R$ between the centers of the nuclei to separate; this is the quasifission. The DNS model thus contains two important new aspects for the complete fusion: (i) the appearance of a specific inner fusion barrier in the mass asymmetry coordinate, which determines the excitation energy of the compound nucleus, and (ii) the competition between complete fusion and quasifission during the time development of the dinuclear system to the compound nucleus. The competing process of quasifission diminishes the fusion probability of very heavy systems by many orders of magnitude. In the DNS model the inner fusion barrier could be smaller than the fusion barrier in the macroscopic models that need an extra-extra push for the fusion and, therefore, give a too high excitation energy of the compound nucleus. It turns out that the DNS is one of a few models so far that gives no contradiction to available experimental data.

One of the open questions is the effect of the nuclear deformation. In principle, the deformed nuclei may have different orientations that can supply different conditions for the synthesis of SHN. And different orientations for a certain kind of projectile-target combination may lead to different quasifission barriers of the incident channel and different inner fusion barriers in the potential energy surfaces for the nucleon transfer within DNS model. The two factors can both influence the production cross sections of SHN. In Ref. [14], it is observed that the deformed target can influence the fusion in a way that collision with side leads to fusion-fission while the collision with tip leads to quasifission. Thus, in this article, we attempt to study the competition between the fusion and the quasifission at different nuclear orientations for some Pb-based cold fusion reactions and study the dependence of the evaporation residue cross sections of SHN on nuclear orientations within DNS model. The article is organized as follows: in Sec. II, a description about the dinuclear system model is presented. Some results about the potential energy surface and SHN production are described in Sec. III. The summary is given in Sec. IV.

## II. DINUCLEAR SYSTEM CONCEPT

### A. Evaporation residue cross section for SHN

In DNS model, it is assumed that the two touching nuclei always keep their individualities, and the compound nucleus can be formed from dinuclear configuration by nucleon transfer from the light nucleus to the heavy one. The dinuclear system may evolve along two degrees of freedom: (i) along the mass asymmetry degree of freedom, $\eta = \frac{A_1 - A_2}{A_1 + A_2}$, and at the extreme asymmetric condition, $\eta = \pm 1$, the compound nucleus formed; and (ii) along the distance $R$ between centers of two nuclei, and the evolution along increasing $R$ will lead to the quasifission of the DNS. The evaporation residue cross

 

section can be written as

$$\sigma_{ER}(E_{\rm cm}) = \sum_{J=0}^{J=J_f} \sigma_c(E_{\rm cm}, J) P_{\rm CN}(E_{\rm cm}, J) W_{\rm sur}(E_{\rm cm}, J), \quad (1)$$

where $\sigma_C$, $P_{\rm CN}$, $W_{\rm sur}$ represent the capture cross section of two colliding nuclei overcoming the potential barrier in the entrance channel to form the DNS, the probability for the dinuclear system to form compound nucleus via nucleon transfer and the survival probability for the compound nucleus in de-excitation process, respectively. The transmission probability is calculated by introducing barrier distribution function, which can reproduce very well available experimental capture cross sections [10,15]. The survival probability is treated by the statistical model [16,17].

The nucleon transfer process can be described with the master equation (ME)

$$\frac{dP(A_1, E_1, t)}{dt} = \sum_{A_1'} W_{A_1, A_1'}[d_{A_1} P(A_1', E_1', t) - d_{A_1'} P(A_1, E_1, t)] - \Lambda^{\rm qf}(\Theta) P(A_1, E_1, t), \quad (2)$$

where $P(A_1, E_1, t)$ denotes the distribution function to find fragment 1 with $A_1$ nucleons and local excitation energy $E_1$ at time $t$. Here $E_1$ is determined by the dissipation energy from the relative motion and the potential energy of the corresponding DNS, which is presented as $\varepsilon_1^*$, and will be shown later in Eqs. (12) and (13). The dissipation energy is described by the parametrization method of the classical deflection function [18,19]. $W_{A_1, A_1'}$ is the mean transition probability from $(A_1, E_1)$ to $(A_1', E_1')$ and $d_{A_1}$ denotes the microscopic dimension for fragment 1 with macroscopic variables $(A_1, E_1)$. The sum should be taken over all mass numbers (from 0 to $A_1 + A_2$). $\Lambda^{\rm qf}(\Theta)$ is the quasifission rate along the variable $R$. The single-particle Hamiltonian to describe the nucleon's motion in dinuclear model reads

$$H(t) = H_0(t) + V(t) \quad (3)$$

$$H_0(t) = \sum_k \sum_{\nu_k} \varepsilon_{\nu_k}(t) a_{\nu_k}^\dagger(t) a_{\nu_k}(t) \quad (4)$$

$$V(t) = \sum_{k,k'} \sum_{\alpha_k, \beta_{k'}} u_{\alpha_k, \beta_{k'}}(t) a_{\alpha_k}^\dagger(t) a_{\beta_{k'}}(t) = \sum_{k,k'} V_{k,k'}(t), \; k, k' = 1, 2, \quad (5)$$

where $k, k'(k, k' = 1, 2)$ denote fragment 1 or 2. $\varepsilon_\nu(t)$ and $u_{\nu\mu}(t)$ are single-particle energy levels and interaction matrix element, respectively [16,20]. The single-particle states are defined with respect to the centers of the interacting nuclei and are assumed to be orthogonalized in the overlap region. So the annihilation and creation operators are dependent on time. The single-particle matrix elements are parameterized by

$$u_{\alpha_K, \beta_{K'}}(t) = U_{K,K'}(t) \times \left( \exp\left\{ -\frac{1}{2} \left[ \frac{\varepsilon_{\alpha_K}(t) - \varepsilon_{\beta_{K'}}(t)}{\Delta_{K,K'}(t)} \right]^2 \right\} - \delta_{\alpha_K, \beta_{K'}} \right), \quad (6)$$

which contains five fixed independent parameters $U_{11}(t)$ and $U_{22}(t)$ for exciting a nucleon in fragments 1 and 2, respectively, and $U_{12}(t) = U_{21}(t)$ for transferring a nucleon between the fragments and the corresponding width parameters $\Delta_{11}(t) = \Delta_{22}(t)$ and $\Delta_{12}(t) = \Delta_{21}(t)$. The detailed calculation of these parameters is described in Refs. [15,16,20]. The strength parameters are given by

$$U_{kk'} = \frac{g_1^{\frac{1}{3}} g_2^{\frac{1}{3}}}{g_1^{\frac{1}{3}} + g_2^{\frac{1}{3}}} \times \frac{1}{g_k^{\frac{1}{3}} g_{k'}^{\frac{1}{3}}} \times 2\gamma_{kk'}, \quad (7)$$

with $g_k = A_k/12$, and the reduced strength parameters $\gamma_{11} = \gamma_{22} = \gamma_{12} = \gamma_{21} = 3$ [15,16,20].

The transition probability reads:

$$W_{A_1, A_1'} = \frac{\tau_{\rm mem}(A_1, E_1, A_1', E_1')}{\hbar^2 d_{A_1} d_{A_1'}} \times \sum_{ii'} |\langle A_1', E_1', i' | V | A_1, E_1, i \rangle|^2, \quad (8)$$

where $i$ denotes all remaining quantum numbers. The memory time is:

$$\tau_{\rm mem}(A_1, E_1; A_1', E_1') = (2\pi)^{1/2} \hbar \left\{ \langle V^2(t) \rangle_{A_1, E_1} + \langle V^2(t) \rangle_{A_1', E_1'} \right\}^{-1/2}, \quad (9)$$

where $\langle \rangle_{A_1, E_1}$ stands for the average expectation value with $A_1, E_1$ fixed. According to Eq. (5), the transition probability can be written as [20,21]:

$$W(A_1, E_1; A_1', E_1') = \frac{\tau_{\rm mem}(A_1, E_1; A_1', E_1')}{d_{A_1} d_{A_1'}} \{ [\omega_{11}(A_1, E_1; E_1') + \omega_{22}(A_1, E_1; E_1')] \delta_{A_1 A_1'} + \omega_{12}(A_1, E_1; E_1') \delta_{A_1', A_1 - 1} + \omega_{21}(A_1, E_1; E_1') \delta_{A_1', A_1 + 1} \}, \quad (10)$$

where

$$\omega_{KK'}(A_1, E_1; E_1') = \sum_{ii'A_1'} |\langle A_1, E_1, i | V_{k,k'} | A_1', E_1', i' \rangle|^2 = d_{A_1} \langle V_{kk'} V_{kk'}^\dagger \rangle. \quad (11)$$

During the reaction process, the relative kinetic energy is gradually dissipated into the intrinsic excitation energy of the nuclei, a valence space $\Delta\varepsilon$ is thus formed symmetrically around the Fermi surface. Only the nucleons in the valence space can be excited or transferred.

$$\Delta\varepsilon_k = \sqrt{\frac{4\varepsilon_k^*}{g_k}}, \quad \varepsilon_k^* = \varepsilon^*(t) \frac{A_k}{A}, \quad g_k = A_k/12, \quad (12)$$

where $\varepsilon^*(t)$ is the local excitation energy of the DNS, which determines the mean transition probability. There are

$N_K = g_K \Delta\varepsilon_K$ valence states and $m_K = N_K/2$ valence nucleons in the valence space $\Delta\varepsilon_K$, which give the dimension

$$d(m_1, m_2) = \binom{N_1}{m_1}\binom{N_2}{m_2}.$$

The local excitation energy of the DNS is defined as

$$\varepsilon^*(t) = E(t) - U(A_1, A_2), \tag{13}$$

where $E(t)$ is the intrinsic excitation energy of the composite system converted from the relative kinetic energy loss, which is determined for each initial relative angular momentum $J$ by the parametrization method of the classical deflection function. The method has been described in detail in Ref. [18]. $U(A_1, A_2)$ is the driving potential energy of the system for the nucleon transfer of the DNS, and will be given in the next section. The transitions for a proton or neutron are not distinguished in the transition probability because the ME is essentially restricted to one dimension. It is, however, remedied by including the explicit proton and neutron numbers of the isotopic composition of the nuclei forming the DNS in the driving potential. The averages in Eqs. (9) and (11) are carried out by using the method of spectral distributions [22–24]. We obtain

$$\langle V_{kk'} V^\dagger_{kk'} \rangle = \frac{1}{4} U^2_{kk'} g_k g_{k'} \Delta_{kk'} \Delta\varepsilon_k \Delta\varepsilon_{k'} \times \left[ \Delta^2_{kk'} + \frac{1}{6}\left(\Delta\varepsilon_k^2 + \Delta\varepsilon_{k'}^2\right)\right]^{-1/2}. \tag{14}$$

The nucleus-nucleus interaction potential as a function of the relative distance $R$ of two nuclei has a pocket with a small depth that results from the attractive nuclear and repulsive Coulomb interactions. The probability $P(A_1, E_1, t)$ distributed in the pocket will have the chance to decay out of the pocket with a decay rate $\Lambda^{\rm qf}_{A_1,E_1,t}(\Theta)$ in the ME. Therefore, the evolution of the DNS along the variable $R$ leads to the quasifission of the DNS. The quasifission rate $\Lambda^{\rm qf}$ can be estimated with the one-dimensional Kramers formula [25]:

$$\Lambda^{\rm qf}[\Theta(t)] = \frac{\omega}{2\pi\omega^{B_{\rm qf}}}\left[\sqrt{\left(\frac{\Gamma}{2\hbar}\right)^2 + (\omega^{B_{\rm qf}})^2} - \frac{\Gamma}{2\hbar}\right] \times \exp\left[-\frac{B_{\rm qf}(A_1, A_2)}{\Theta(t)}\right]. \tag{15}$$

Here the quasifission barrier $B_{\rm qf}$ measures the depth of the pocket of the interaction potential. The local temperature is given by the Fermi-gas expression $\Theta = \sqrt{\varepsilon^\star/a}$ corresponding to the local excitation energy $\varepsilon^\star$ and level-density parameter $a = A/12$ MeV$^{-1}$. $\omega^{B_{\rm qf}}$ is the frequency of the inverted harmonic oscillator approximating the interaction potential of two nuclei in $R$ around the top of the quasifission barrier, and $\omega$ is the frequency of the harmonic oscillator approximating the potential in $R$ at the bottom of the pocket. The quantity $\Gamma$ denotes the double average width of the contributing single-particle states. According to the linear response theory by Hofmann *et al.* [26], the friction coefficients are simply approximated by $\gamma_{ii'} = \frac{\Gamma}{\hbar}\mu_{ii'}$, (with $i, i' = R, \eta$). In Ref. [27], it is argued that the friction coefficients $\gamma_{RR}$ and $\gamma_{\eta\eta}$ obtained with $\Gamma = 2.8$ MeV has the same order of magnitude as the one calculated within the one-body dissipation model by Ref. [28]. So, the value $\Gamma = 2.8$ MeV is used. Here we use average constant values $\hbar\omega^{B_{\rm qf}} = 2.0$ MeV and $\hbar\omega = 3.0$ MeV for the following reactions. The Kramers formula is derived at the quasistationary condition of the temperature $\Theta(t) < B_{\rm qf}(A_1, A_2)$. However, the numerical calculation in Ref. [25] indicated that Eq. (15) is also available at the condition of $\Theta(t) > B_{\rm qf}(A_1, A_2)$.

The distribution function $P(A_1, E_1, t)$ can be obtained by solving the master equation numerically. All the configurations on the left side of the BG point [top point on the potential energy surface (PES)] are considered to form the compound nucleus inevitably. Thus the fusion probability $P_{\rm CN}$ can be written as summation of $P(A, E, t)$ from 0 to $A_{\rm BG}$.

$$P_{\rm CN} = \int_{A=0}^{A_{\rm BG}} P(A, E, t) dA \tag{16}$$

### B. Potential energy surface (the driving potential)

The PES is very important in the DNS model, which gives information about the optimal projectile-target combination, optimal excitation energy and influences the fusion probability significantly. The potential energy surface for the nucleon transfer of the DNS is defined as

$$U(A_1, A_2) = U_{\rm LD}(A_1) + U_{\rm LD}(A_2) + V(A_1, A_2) - \left[U^{\rm com}_{\rm LD} + V'_{\rm rot}(J, A)\right], \tag{17}$$

$$V(A_1, A_2) = V_C(A_1, A_2) + V_N(A_1, A_2) + V_{\rm rot}(J), \tag{18}$$

where $U_{\rm LD}(A_1)$, $U_{\rm LD}(A_2)$, and $U^{\rm com}_{\rm LD}$ are the nuclear masses for the fragment 1, fragment 2, and the compound nucleus, respectively. $V_C(A_1, A_2)$, $V_N(A_1, A_2)$, and $V_{\rm rot}(J)$ are the nuclear, Coulomb, and centrifugal parts of the nucleus-nucleus potential, respectively.

The Coulomb interaction can be calculated numerically as follows [29]

$$V_C(A_1, A_2) = \frac{Z_1 Z_2 e^2}{R} + \left(\frac{9}{20\pi}\right)^{\frac{1}{2}}\left(\frac{Z_1 Z_2 e^2}{R^3}\right)\sum_{i=1}^{2} R_i^2 \beta_i P_2(\cos\theta_i) + \left(\frac{3}{7\pi}\right)\left(\frac{Z_1 Z_2 e^2}{R^3}\right)\sum_{i=1}^{2} R_i^2 [\beta_i P_2(\cos\theta_i)]^2, \tag{19}$$

where $R_i$, $\beta_i$ are the radius and the quadrupole deformation of the $i$th nucleus, respectively. $\theta_i$ is the angle between radius vector $\vec{R}$ and the symmetry axis of the $i$th nucleus.

As for the nuclear interaction potential, the Skyrme-type interaction without considering the momentum and spin dependence is adopted.The sudden approximation is assumed.

Thus the nuclear potential can read as

$$V_N(A_1, A_2) = C_0\left\{\frac{F_{\rm in} - F_{\rm ex}}{\rho_{00}}\left[\int \rho_1^2(\vec{r})\rho_2(\vec{r}-\vec{R})d\vec{r} + \int \rho_1(\vec{r})\rho_2^2(\vec{r}-\vec{R})d\vec{r}\right] + F_{ex}\int \rho_1(\vec{r})\rho_2(\vec{r}-\vec{R})d\vec{r}\right\} \quad (20)$$

with

$$F_{\rm in,ex} = f_{\rm in,ex} + f'_{\rm in,ex}\frac{N_1 - Z_1}{A_1}\frac{N_2 - Z_2}{A_2}. \quad (21)$$

Here, $N_{1,2}$ and $Z_{1,2}$ are neutron and proton numbers of the two nuclei, respectively. In this work, some parameters are as follows: $C_0 = 300$ MeV fm$^3$, $f_{\rm in} = 0.09$, $f_{\rm ex} = -2.59$, $f'_{\rm in} = 0.42$, $f'_{\rm ex} = 0.54$, and $\rho_{00} = 0.17$ fm$^{-3}$. $\rho_1$ and $\rho_2$ are two-parameter Woods-Saxon density distributions for the two nuclei [30,31]. The distance $R$ between centers of nuclei is taken to be the value which gives the minimum value of $V_C(A_1, A_2) + V_N(A_1, A_2)$.

The evolution of the DNS in the variable $R$ of the relative distance between the centers of the interacting nuclei will lead to the quasifission of the DNS. For a given mass asymmetry $\eta$, the nucleus-nucleus interaction potential as a function of $R$ is:

$$V(A_1, A_2, R) = V_C(A_1, A_2, R) + V_N(A_1, A_2, R) + V_{\rm rot}(A_1, A_2, R), \quad (22)$$

where the Coulomb interaction $V_C$ and the nuclear interaction $V_N$ are as a function of $R$ at each combination of the DNS. $V_{\rm rot}$ is the centrifugal potential. The nucleus-nucleus interaction potential $V(A_1, A_2, R)$ has a pocket as a function of the relative distance $R$ with a small depth that results from the attractive nuclear and repulsive Coulomb interactions. The probability $P(A_1, E_1, t)$ distributed in the pocket will have the chance to decay out of the pocket with a decay rate $\Lambda^{\rm qf}_{A_1,E_1,t}(\Theta)$ in the ME.

## III. RESULTS

### A. The influence of orientation on the potential energy surface

As mentioned above, the PES, which governs the nucleon transfer, can be calculated with Eq. (17), where the distance $R$ between the centers of nuclei is chosen as the value that gives the minimum value of $V_C(A_1, A_2, R) + V_N(A_1, A_2, R)$. The PES for the reactions $^{58}$Fe + $^{208}$Pb, $^{70}$Zn + $^{208}$Pb, $^{82}$Se + $^{208}$Pb and $^{86}$Kr + $^{208}$Pb are shown in Figs. 1(a), 1(b), 1(c)

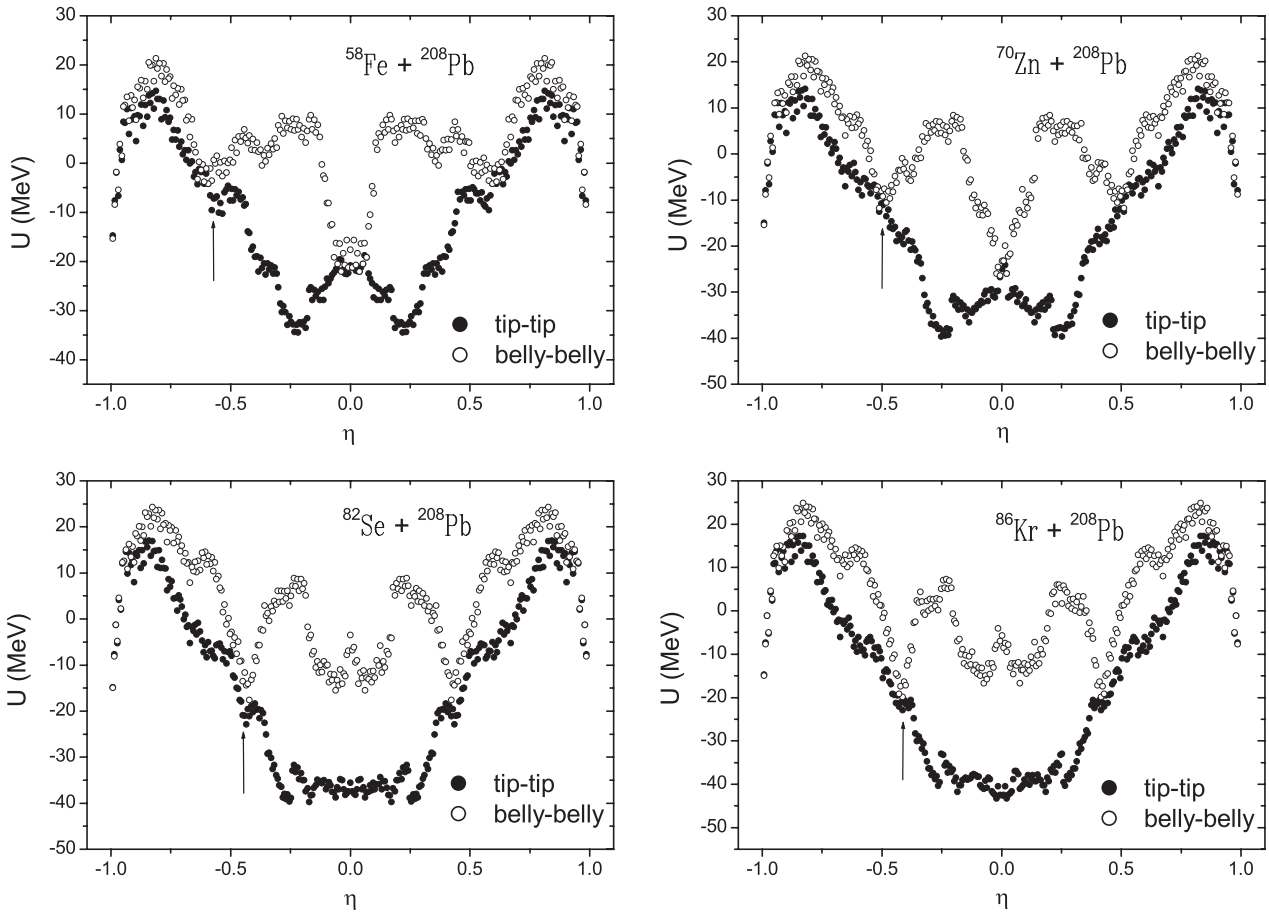


FIG. 1. Potential energy surfaces for (a) $^{58}$Fe + $^{208}$Pb, (b) $^{70}$Zn + $^{208}$Pb, (c) $^{82}$Se + $^{208}$Pb, and (d) $^{86}$Kr + $^{208}$Pb as functions of mass asymmetry. The solid circles represent the PES at tip-tip nuclear orientation, whereas the open circles represent the PES at belly-belly nuclear orientation.

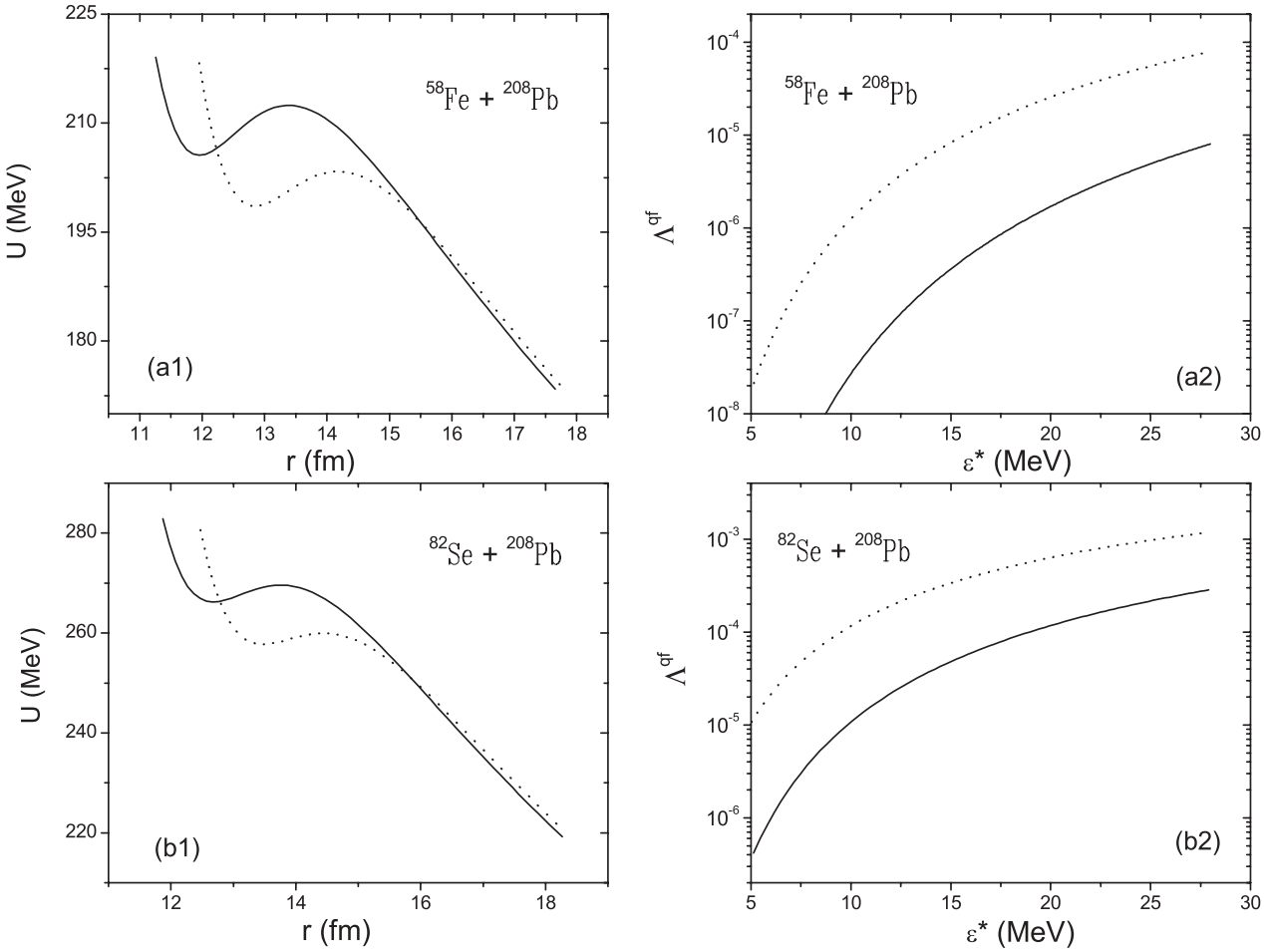


FIG. 2. Interaction potentials for (a1) $^{58}$Fe + $^{208}$Pb and (b1) $^{82}$Se + $^{208}$Pb as functions of central distance between two nuclei, and quasifission rates for (a2) $^{58}$Fe + $^{208}$Pb, (b2) $^{82}$Se + $^{208}$Pb as functions of excitation energies of dinuclear system. Dotted lines are for the tip-tip case and solid lines are for the belly-belly case.

and 1(d), respectively. The PESs at tip-tip and belly-belly orientations are displayed. In each figure the solid circles (curve 1) represent the tip-tip case, and open circles (curve 2) represent the belly-belly case. If we make comparison between the curve 1 and curve 2, it is found that the shapes of PES for the two orientations are quite different. Generally, for the belly-belly orientations, a barrier can be found between $\eta \sim -0.3$ and $\eta \sim -0.2$ on the right side of the incident configuration, and here we call it $B_{\rm sy}$. In Fig. 1(a) the incident channel is at $\eta = -0.56$, one may see that the potential energy for incident configuration is located in an energy pocket between the inner fusion barrier $B_{\rm inner}$ and $B_{\rm sy}$. For the tip-tip case, the barrier $B_{\rm sy}$ on the right side of the incident configuration is rather low (about 2.53 MeV) but the inner fusion barrier is about 21.88 MeV. However, for the belly-belly case, the inner fusion barrier $B_{\rm inner}$ is 21.37 MeV and the barrier $B_{\rm sy}$, which hinders the nucleon diffusion toward the symmetrical configuration, is about 9.74 MeV. Thus, for the two cases, inner fusion barriers are nearly the same, but the barriers $B_{\rm sy}$ are quite different. For the belly-belly case, more probabilities may be stored in the pocket, which may enhance the fusion. Furthermore, with decreasing the absolute value of mass asymmetry $|\eta|$, the quasifission barrier decreases so the quasifission rate increases. One may bear in mind that the fraction of the probability, which goes to quasifission, leaks out of the evolution system, so the decay in $R$ affects the motion of the system in $\eta$. With higher $B_{\rm sy}$ less probability distributes to the symmetrical region to undergo quasifission, the effect also enhances the fusion. For the tip-tip case, the nucleon diffusion to the symmetric direction is much easier due to the lower $B_{\rm sy}$, and the quasifission could be more pronounced. One may find the similar schema in Figs. 1(b), 1(c), and 1(d). The detailed inner fusion barrier and $B_{\rm sy}$ for some reaction channels are listed in Table I. This description is agreeable with the conclusion in Ref. [14] that belly-belly collisions lead to fusion, whereas collision with tips lead to quasifission.

Our calculations claim that for the reaction $^{82}$Se + $^{142}$Ce with $E_{\rm cm}$ around $V_B$, the fusion probabilities at belly-belly case and tip-tip case are $4 \times 10^{-3}$ and $2 \times 10^{-3}$, respectively. The probability at belly-belly is about twice of that at tip-tip case. For the reaction $^{76}$Ge + $^{150}$Nd, because of the strong prolate deformation of $^{150}$Nd, the fusion probability at belly-belly is five times larger than that at the tip-tip case. And it is found that fusion probability for $^{76}$Ge + $^{150}$Nd is larger than that for $^{82}$Se + $^{142}$Ce. Actually, the reason can be attributed to two

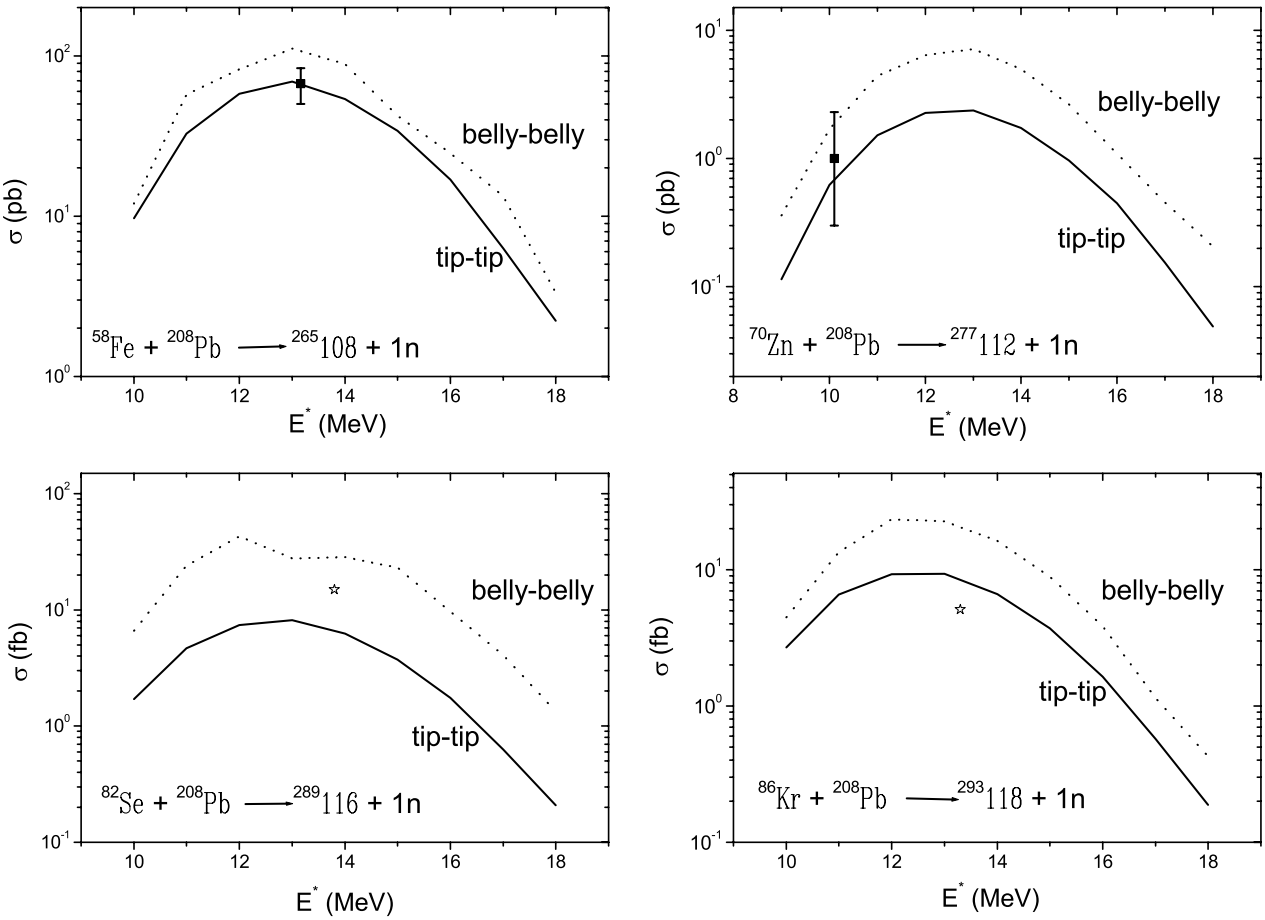


FIG. 3. The excitation functions for (a) $^{58}\mathrm{Fe} + {}^{208}\mathrm{Pb} - {}^{265}108 + 1n$, (b) $^{70}\mathrm{Zn} + {}^{208}\mathrm{Pb} - {}^{277}112 + 1n$, (c) $^{82}\mathrm{Se} + {}^{208}\mathrm{Pb} - {}^{289}116 + 1n$, and (d) $^{86}\mathrm{Kr} + {}^{208}\mathrm{Pb} - {}^{293}118 + 1n$. The solid lines represent the tip-tip case, and the dotted lines represent the belly-belly case. The experimental data are depicted with solid dot, together with error bars. In lower figures, the star represents the calculation results from Adamian *et al.* [8]

factors. On one hand, it is the effect of the nuclear deformation and orientation. On the other hand, the mass asymmetry for $^{76}\mathrm{Ge} + {}^{150}\mathrm{Nd}$ ($\eta_1 = -0.3274$) is smaller than that for $^{82}\mathrm{Se} + {}^{142}\mathrm{Ce}$ ($\eta_2 = -0.2679$), which may also contribute to the difference.

### B. The quasifission and evaporation residue cross sections

The nucleus-nucleus interaction potentials as a function of the relative distance between the centers of the interacting nuclei $R$ for the dinuclear configuration $^{58}\mathrm{Fe} + {}^{208}\mathrm{Pb}$ and $^{82}\mathrm{Se} + {}^{208}\mathrm{Pb}$ channels are depicted in Figs. 2(a1) and 2(b1), respectively. As shown in Fig. 2(a1), the height of the barrier at belly-belly orientation is 9.1 MeV higher than that at tip-tip case. Thus, at a certain bombarding energy, the lower excitation energy can be obtained at belly-belly orientation. It can be also found that the quasifission barrier at belly-belly orientation is 2 MeV higher than that at the tip-tip case. Thus, at a certain bombarding energy, the lower quasifission rate may be obtained at belly-belly case because of the lower excitation energy and higher quasifission barrier. The corresponding quasifission rates to overcome the barriers at belly-belly orientation (solid line) and at tip-tip orientation (dotted line) as functions of dinuclear system excitation energy are shown in Figs. 2(a2) and 2(b2), respectively. It is found in Figs. 2(a2) that the quasifission rates at two orientations are increasing with the excitation energy. But the rate at the tip-tip case is much larger (about one order of magnitude or even larger) than that at the belly-belly case. In Figs. 2(b2), the rate at the tip-tip case is also larger (from four times to one order of magnitude) than that at the belly-belly case. And the difference between the quasifission rates at two orientations for $^{58}\mathrm{Fe} + {}^{208}\mathrm{Pb}$ seems larger than that for $^{82}\mathrm{Se} + {}^{208}\mathrm{Pb}$, because the difference between the quasifission barrier heights at two orientations for the relatively heavier dinuclear system is smaller than that for the relatively lighter dinuclear system.

TABLE I. The inner fusion barrier $B_{\mathrm{inner}}$ and barrier $B_{\mathrm{symmetry}}$ for some Pb-based reaction channels.

| Projectile | $B_{\mathrm{sy}}^{t-t}$ (MeV) | $B_{\mathrm{inner}}^{t-t}$ (MeV) | $B_{\mathrm{sy}}^{b-b}$ (MeV) | $B_{\mathrm{inner}}^{b-b}$ (MeV) |
|---|---|---|---|---|
| $^{54}$Cr | 5.18 | 21.43 | 11.92 | 22.11 |
| $^{58}$Fe | 2.53 | 21.88 | 9.74 | 21.37 |
| $^{70}$Zn | 0.64 | 25.20 | 17.49 | 30.46 |
| $^{76}$Ge | 0.83 | 33.16 | 19.36 | 33.27 |
| $^{82}$Se | 4.60 | 39.97 | 23.33 | 38.68 |
| $^{86}$Kr | 2.47 | 40.28 | 27.18 | 44.71 |

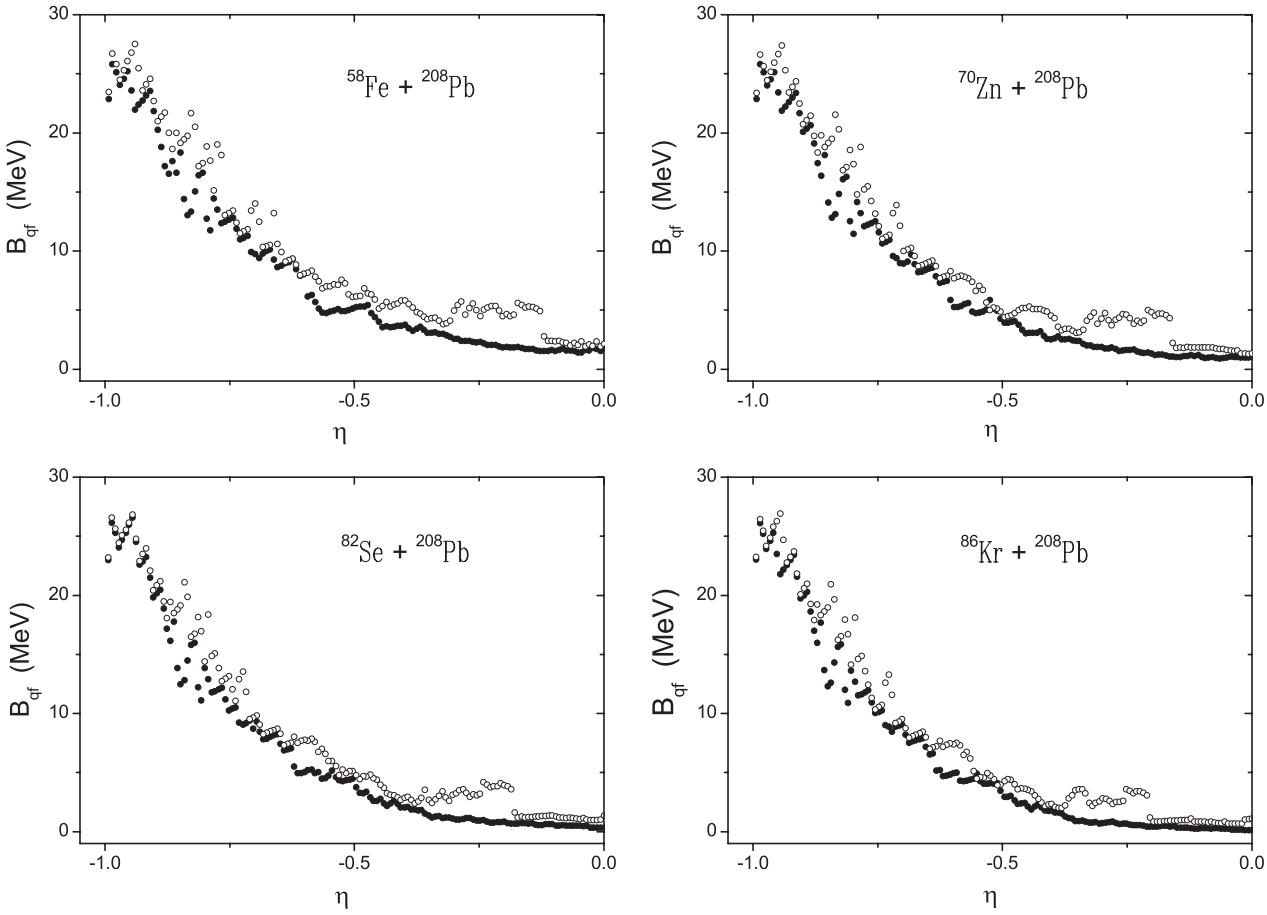


FIG. 4. The quasi fission barriers for (a) $^{58}$Fe + $^{208}$Pb − $^{265}$108 + 1$n$, (b) $^{70}$Zn + $^{208}$Pb − $^{277}$112 + 1$n$, (c) $^{82}$Se + $^{208}$Pb − $^{289}$116 + 1$n$ and (d) $^{86}$Kr + $^{208}$Pb − $^{293}$118 + 1$n$. The solid circles represent the tip-tip case while the open circles represent the belly-belly case.

By solving the master equation coupled with the relative motion, the fusion probability can be obtained. After the formation of the compound nucleus, it will de-excite by means of fission or emitting small number of neutron. Thus, the competition between the fission and the emission of neutron can determine the survival probability of the SHN. Then, for the cold fusion reaction the survival probability can be written as

$$W_{\rm sur}(E^*, J) = P_1(E^*, J)\frac{\Gamma_n(E^*, J)}{\Gamma_n(E^*, J) + \Gamma_f(E^*, J)}, \quad (23)$$

where the $E^*$, $J$ are excitation energy and angular momentum of the compound nuclei. The $P_1(E^*, J)$ represents the realization probability, and $\Gamma_n$, $\Gamma_f$ stand for the neutron emission width and fission width, respectively. The neutron emission width and fission width can, respectively, read

$$\Gamma_n(E^*) = \frac{1}{2\pi\rho(E^*)} \times \frac{2M_nR^2}{\hbar^2} g \int_0^{E^*-B_n-1/a} \varepsilon\rho(E^* - B_n - \varepsilon)\, d\varepsilon \quad (24)$$

and

$$\Gamma_f(E^*) = \frac{1}{2\pi\rho(E^*)} \int_0^{E^*-B_f-1/a} \rho(E^* - B_f - \varepsilon)\, d\varepsilon, \quad (25)$$

where $\rho(E^*) = \frac{1}{\sqrt{48E^*_{\rm CN}}} \exp[2\sqrt{aE^*_{\rm CN}}]$ is the energy level density with the level-density parameter $a$, $M_n$ stands for the mass of neutron, $R$, $B_n$, $B_f$ represent the radius, neutron separation energy and fission barrier of the compound nucleus, respectively. The neutron separation energies are taken from Ref. [32]. The fission barrier can be separated into two parts, the macroscopic part $B_f^{\rm LD}$ and the microscopic part $B_f^{\rm mic}$ as [11,16,33]

$$B_f = B_f^{\rm LD} + B_f^{\rm mic} \exp\left[-\frac{E^*}{E_D}\right], \quad (26)$$

where $E_D$ is the damping factor because the microscopic part comes from the shell energy, which is decreasing with increasing the excitation energy of the compound nucleus.

Applying Eq. (1), we can obtain the evaporation residue cross sections for the superheavy nuclei. The excitation functions for the cold fusion reactions $^{58}$Fe + $^{208}$Pb − $^{265}$108 + 1$n$, $^{70}$Zn + $^{208}$Pb − $^{277}$112 + 1$n$, $^{82}$Se + $^{208}$Pb − $^{289}$116 + 1$n$, and $^{86}$Kr + $^{208}$Pb − $^{293}$118 + 1$n$ are shown in Fig. 3. The experimental results are shown in upper figures with a solid dot together with an error bar. For the heavy projectile $^{82}$Se and $^{86}$Kr, no experimental data are available. The results from Adamian *et al.* are shown with stars. When comparing the residue cross sections at two orientations, it is seen that at

belly-belly orientation, the residue cross section is larger than those at tip-tip orientation. The quasifission barriers for the corresponding channels are shown as a function of mass asymmetry $\eta$ in Fig. 4. It is indicated that the quasifission barrier for the belly-belly case is bigger than that for the tip-tip case, which suppresses quasifission and thus helps fusion.

And, in general, for the relatively lighter projectile, the residue cross-section difference between the two orientations is small, e.g., for the $^{58}\mathrm{Fe} + {}^{208}\mathrm{Pb} - {}^{265}108 + 1n$ reaction, the difference is about 1.5 times. However, for the relatively heavier projectile, e.g., for $^{82}$Se, $^{86}$Kr, the difference between two orientations can be larger, about 3–4 times. We can conclude that the belly-belly orientation, at which the target and projectile can reach each other in a more compact way, is in favor of the production of the superheavy nuclei than that of tip-tip orientation.

## IV. SUMMARY

In summary, the PES, the evaporation residue cross sections at tip-tip and belly-belly nuclear orientations for some cold fusion reactions leading to superheavy elements are calculated. Because at belly-belly orientation the barrier that prevents the DNS system from moving to more symmetric configurations where the DNS system will be more likely to decay by means of quasifission and the quasifission barrier are both higher than those at tip-tip orientation, it is found that the evaporation residue cross sections of superheavy nuclei at belly-belly orientation are larger than those at tip-tip orientation, and thus the belly-belly orientation is in favor of the production of SHN.

## ACKNOWLEDGMENTS

The work was supported by the Natural Science Foundation of China under grant nos. 10505016, 10775061, 10475099, 10435010, 10705014, and 10575036. The Knowledge Innovation Project of the Chinese Academy of Sciences under grant nos. KJCX2-SW-N17 and KJCX3-SYW-N02, a major state basic research development program under grant no. 2007CB815000; and support from the DFG of Germany.

[1] S. Hofmann and G. Münzenberg, Rev. Mod. Phys. **72**, 733 (2000).
[2] Yu. Oganessian, J. Phys. G: Nucl. Part. Phys. **34**, R165 (2007); S. Hofmann, D. Ackermann *et al.*, Eur. Phys. J. A **32**, 251 (2007).
[3] V. V. Volkov, Izv. Akad. Nauk SSSR, Ser. Fiz. **50**, 1879 (1986).
[4] N. V. Antonenko, E. A. Cherepanov, A. K. Nasirov, V. P. Permjakov, and V. V. Volkov, Phys. Lett. **B319**, 425 (1993); Phys. Rev. C **51**, 2635 (1995).
[5] E. A. Cherepanov, V. V. Volkov, N. V. Antonenko, and A. K. Nasirov, in *Proceedings of International Symposium on Heavy-Ion Physics and its Applications, 29 August–1 September, 1995, Lanzhou, China* (World Scientific Publishing Co. Pte. Ltd., 1996), pp. 272–282.
[6] G. G. Adamian, N. V. Antonenko, and W. Scheid, Nucl. Phys. **A618**, 176–198 (1997).
[7] G. G. Adamian, N. V. Antonenko, W. Scheid, and V. V. Volkov Nucl. Phys. **A627**, 361 (1997).
[8] G. G. Adamian, N. V. Antonenko, and W. Scheid, Nucl. Phys. **A678**, 24–38 (2000).
[9] Y. Aritomo, T. Wada, M. Ohta, and Y. Abe, Phys. Rev. C **59**, 796 (1999).
[10] V. I. Zagrebaev, Phys. Rev. C **64**, 034606 (2001).
[11] V. I. Zagrebaev, Y. Aritomo, M. G. Itkis, Yu. Ts. Oganessian, and M. Ohta, Phys. Rev. C **65**, 014607 (2001).
[12] W. J. Swiatecki, Phys. Scr. **24**, 113 (1981); S. Bjørnholm and W. J. Swiatecki, Nucl. Phys. **A391**, 471 (1982).
[13] J. Blocki, H. Feldmeier, and W. J. Swiatecki, Nucl. Phys. **A459**, 145 (1986).
[14] K. Nishio, H. Ikezoe, S. Mitsuoka, K. Satou, and S. C. Jeong, Phys. Rev. C **63**, 044610 (2001).
[15] Z. Q. Feng, G. M. Jin, F. Fu, and J. Q. Li, Nucl. Phys. **A771**, 50 (2006).
[16] W. Li, N. Wang *et al.*, J. Phys. G: Nucl. Part. Phys. **32**, 1143 (2006).
[17] A. S. Zubov, G. G. Adamian, N. V. Antonenko, S. P. Ivanova, and W. Scheid, Phys. Rev. C **65**, 024308 (2002).
[18] G. Wolschin and W. Nörenberg, Z. Phys. A **284**, 209 (1978).
[19] J.-Q. Li and G. Wolschin, Phys. Rev. C **27**, 590 (1983).
[20] W. F. Li, N. Wang, and J. F. Li *et al.*, Europhys. Lett. **64**, 750 (2003).
[21] J. Q. Li, H. S. Xu, W. Zuo, J. F. Li, and W. Li, in *Proceedings of CCAST-WL Workshop on Radioactive Nuclear Beam Physics, 2001, Beijing, China* (2002), Vol. 138, p. 41.
[22] J. B. French and K. F. Ratcliff, Phys. Rev. C **3**, 94 (1971).
[23] F. S. Chang, J. B. French, and T. H. Thio, Ann. Phys. **66**, 137 (1971).
[24] S. Ayik and J. N. Ginocchio, Nucl. Phys. **A221**, 285 (1974); Nucl. Phys. **A234**, 13 (1974).
[25] P. Grange, J. Q. Li, and H. A. Weidenmüller, Phys. Rev. C **27**, 2063 (1983).
[26] H. Hofmann and P. J. Siemens, Nucl. Phys. **A257**, 165 (1976); **A275**, 464 (1977).
[27] G. G. Adamian, N. V. Antonenko, and W. Scheid, Phys. Rev. C **68**, 034601 (2003).
[28] W. U. Schroeder and J. R. Huizenga, in *Treatise on Heavy-Ion Science*, edited by D. A. Bromley (Plenum Press, New York, 1984), Vol. 2, p. 115.
[29] C. Y. Wong, Phys. Rev. Lett. **31**, 766 (1973).
[30] Q. Li, W. Zuo, and W. Li *et al.*, Eur. Phys. J. A **24**, 223 (2005).
[31] G. G. Adamian, N. V. Antonenko, and R. V. Jolos *et al.*, Int. J. Mod. Phys. E **5**, 191 (1996).
[32] P. Möller, J. R. Nix, W. D. Myers, and W. J. Swiatecki, At. Data Nucl. Data Tables **59**, 185 (1995).
[33] W. F. Li, Z. Z. Wang *et al.*, Chin. Phys. Lett. **21**, 636 (2004).